Measuring a Gas Turbines Parameters and Modeling its Thermodynamic Cycle

Betreut von Patrick Polte, M.Sc.

Lehrstuhl für Turbomaschinen und Flugantriebe

Eingereicht von Cicolini Luisa

Mull Christopher

Vavra Vojtech

Eingereicht am Datum 28.01.2020

Contents

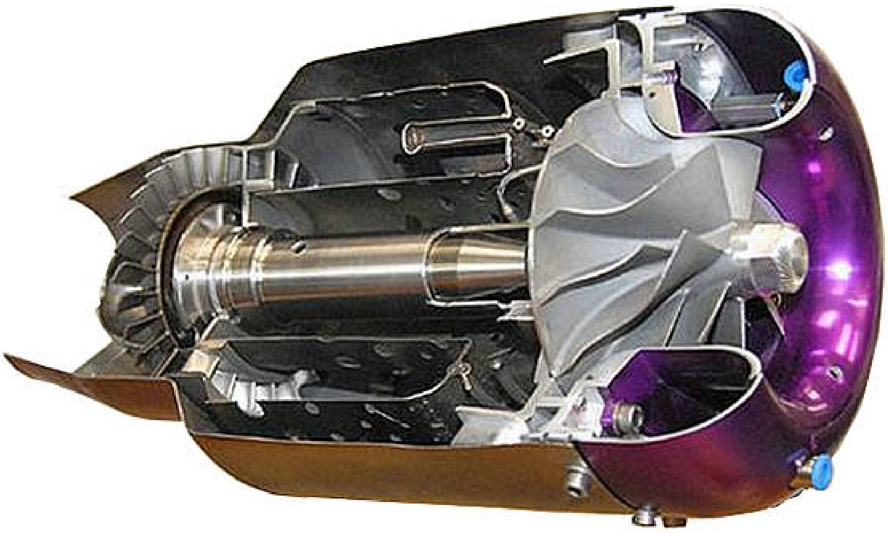

Figure 1: *The Engine used during the experiment*

1 Introduction

Small gas turbines, or micro gas turbines are an ideal test bench for experimental purposes, since their fluid-mechanical and thermodynamic behaviour is analogous to larger gas turbines used in civil as well as military applications[1]. Furthermore, military applications may use the advantages of micro gas turbines, such as the high energy density potential in comparison to similar battery power systems, thus reducing weight and improving operational flexibility as well[2]. For this internship, a small TJ 70 turbine is set on a test bench and measurements are performed with the goal of recalculating its thermodynamic cycle in an accurate way and evaluating the measurements and the system model by applying basic thermodynamic models.

2 Engine Description

The tested micro gas turbine is a JetCat TJ 70 Raptor with 190 N thrust, widely used as RC aircraft engine with a maximum of 120 000 rpm. EGT is 650-700℃ and the fuel is kerosene or petroleum mixed with oil: thanks to its fuel based bearing lubrication there is no need for an additional oil lubrication system. Its specific fuel consumption is about 0.65 l/min[3]. A brushless motor mounted at the inlet acts as a starter and the electrical fuel pump is controlled by a specially designed ECU, offering the possibility of automatic start using kerosene combined with a glow plug. In addition, the tested micro gas turbine is equipped with a protective cage in front of the inlet and different sensors for temperature, engine speed and other parameters. The biggest differences compared to larger turbines are on one hand the small number of compressor and turbine stages - just one of each in TJ 70 - and on the other hand the relatively large combustion chamber with fuel injection tubes.

3 Test Rig and Measurement Procedures

The engine is mounted on a mobile test rig featuring a control panel and monitoring displays. The turbine itself is installed on a small movable platform pointing to a force measuring device. The kerosene supply tank is located under the table. The fuel line is divided in two, one heading towards the ignition system, the other heading to the bearings (with approximately 5% of fuel mass flow). After the bearings, the diverted fuel is added back to the main flow in between the turbine stator and rotor. Finally, all the measured data are recorded using a laptop.

Overall, two separate static test runs are performed, each beginning with the automatic engine startup. When stabilized at idle (approximately 36000 rpm) the first data set is measured during a 10-second interval, at a rate of 25 Hz. Afterwards, the engine speed is increased by increments of 20000 until the maximum speed of 100000 rpm is reached. Finally, the engine is taken back to idle in the same manner, covering the same data set. For every test run, at least three people are required: one controlling the engine throttle, one recording the data and one as observer ready to intervene in abnormal situations.

As a result, 9 datasets are gained for each static run, via different measurement devices, while the ambient data are taken from the TUM weather station located approximately 300 m from the experiment location. Specifically temperature, pressure, force and volumetric flow measurements are obtained during the experiment. As part of the task objectives, one specific measuring technique is described below: the Coriolis mass flow measurement method, which is chosen for detailed description despite not being used during this particular experiment. It may although be in theory an appropriate method for measuring the fuel mass flow in this case.

Figure 2: *Test Rig used for the experiment*

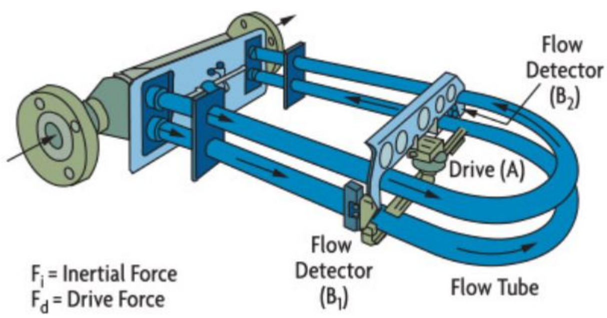

Figure 3: *Coriolis sensor*

4 Coriolis Mass Flow Measurement

The Coriolis force is a virtual force - similar to the centrifugal force - affecting objects involved in circumferential and radial movements at the same time due to the difference in circumferential velocities on different radii. Since this force is directly proportional to the mass, the Coriolis measurement method is a direct method to measure mass flow. The Coriolis mass flow sensor leads the mass flow through a loop route. On one end, an oscillation is induced by an external actuator. This oscillation will alternately induce positive and negative moments: mass flow coming through the sensor line is thus affected by the induced moment.

Due to the different distances from the rotational axis, different circumferential speeds are induced on each fluid element, but when the fluid elements are moving through the pipe further from the rotational axis, their circumferential speeds do not match their original ones any more. This results in a force - the Coriolis force. Similarly, the same effect happens in the opposite direction when fluid elements are flowing back towards the rotational axis on the other side of the sensor. These forces leads to a second oscillation normal to the original externally induced. This second oscillation - induced by the Coriolis force and therefore dependent on mass - is measured by the torque-meter and is used to directly evaluate mass flow.

5 Results

Each dataset from each static run is processed from statistical point of view, resulting in mean value and an error bar representing +/- 1 standard deviation for each of the measurement points (see Figure 4). Engine speed is set manually, the measurement points therefore do not precisely match, but rather form a cluster of points around the given engine speed as seen in the graphs. All measured variables are plotted against the engine speed. As mentioned above, the list of measured variables is as follows:

- Temperatures at compressor outlet, turbine inlet and at nozzle outlet (Figure 4),
- Pressure at compressor outlet (Figure 5),
- Volumetric flow for air at inlet (Figure 6) and of fuel flow (Figure 7),
- Force (thrust) measurement (Figure 8).

The measurements are coupled with ambient temperature and ambient pressure values obtained from the weather station.

Figure 4 shows the obtained temperature probe data: while there is small change in the total temperature at compressor and nozzle outlet, temperature at turbine inlet increases more significantly with engine speeds. Temperature measurements are in accordance with expectations, showing highest values for turbine inlet temperature, followed by nozzle outlet and compressor outlet. Turbine inlet temperature maximum values are noticeably high, as is further discussed in the Discussion.

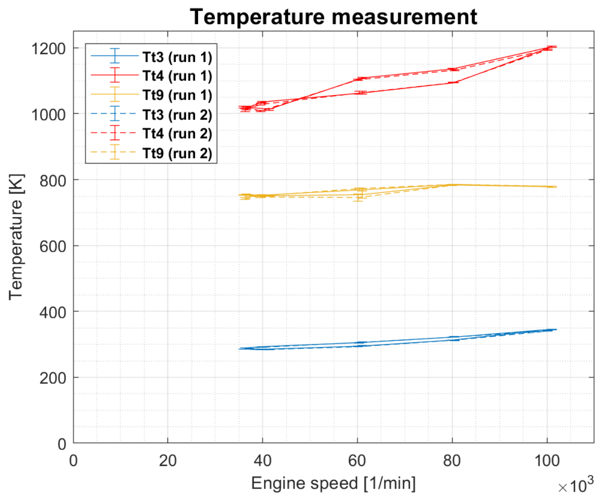

Figure 4: *Temperature Measurement*

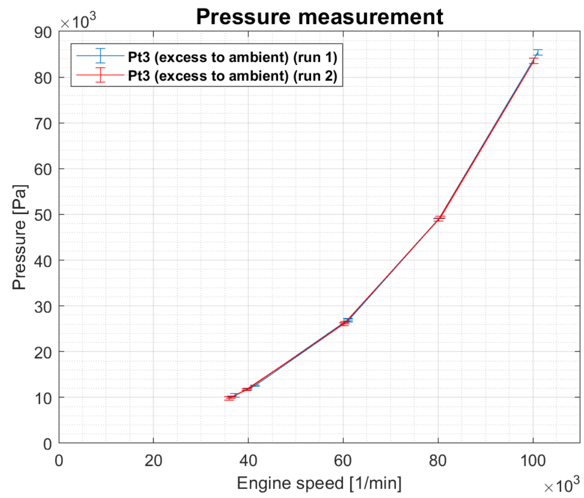

Figure 5: *Pressure Measurement*

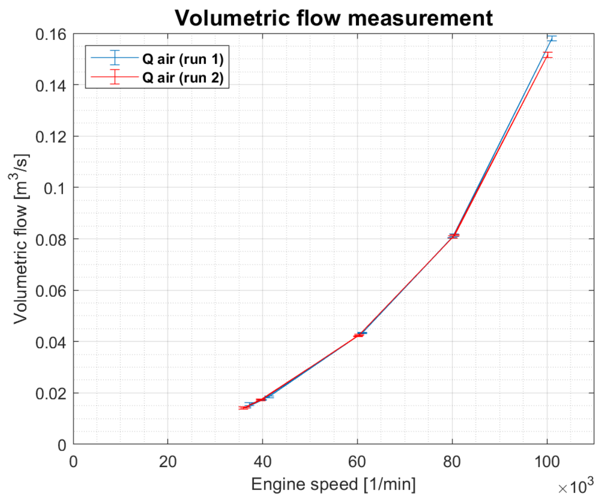

Figure 6: *Air Volume Flow Measurement*

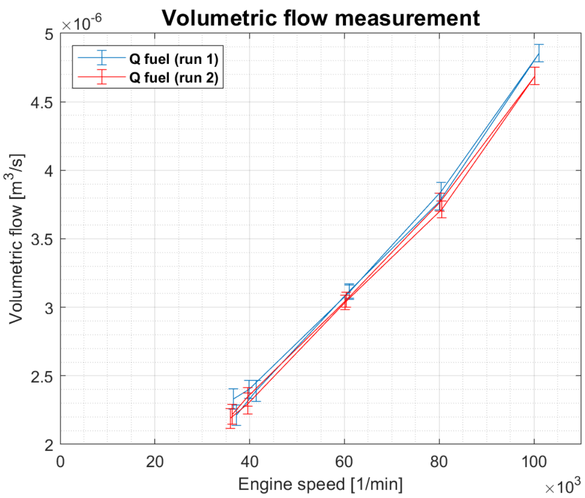

Figure 7: *Fuel Volume Flow Measurement*

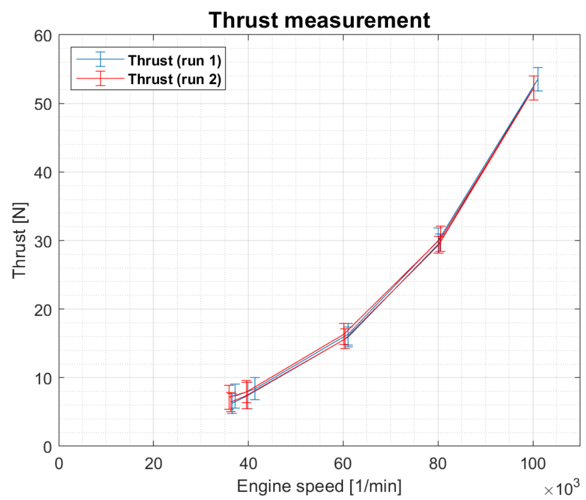

Figure 8: *Thrust Measurement*

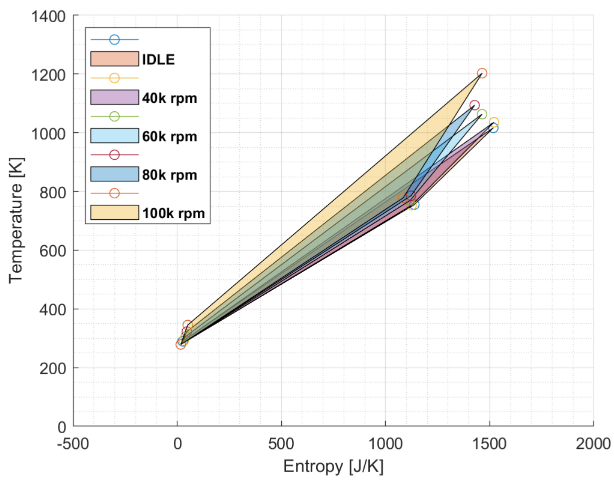

Figure 9: *Cycle Representation*

Further on, Figure 5 shows the total pressure measured after the compressor. Pressure measurement values are recorded as excess to ambient pressure with maximum values thus reaching just under 2 bar. Volumetric flow measurements are depicted separately (Figure 6 and Figure 7) due to the high difference in magnitudes of each variable.

Thrust measurements plotted in Figure 8 reach maximum values above 50N, which is significantly less than manufacturer-specified maximum thrust of 190N, it is however important to keep in mind that the engine speed is only brought up to approx. 80%. What is noticeable are the fairly high readings at near-idle engine speeds.
Across all measured variables, an increase in quantity is observed with higher engine speed, as expected. It is also evident that the error bars are relatively small compared to the measured quantities. Finally, measurement points during run-up and run-down, as well as between each run, are very similar, suggesting confidence in the repeatability of the experiment.

6 Modeling Process

To recalculate the thermodynamic process of the turbine, several assumptions are made to simplify the calculation. The ideal cycle process used for modelling the thermodynamic behavior of a turbojet gas turbine is the Joule-Brayton cycle. This includes an isentropic compression at the beginning, an isobaric heat addition during combustion and an isentropic expansion in the turbine until the nozzle entrance. The remaining difference between the nozzle total pressure and ambient pressure is then used for accelerating the stream of the gas in the nozzle in order to produce thrust.

Nevertheless, in the real case compression and expansion are not isentropic and the heat addition in the combustion chamber is always combined with a slight pressure loss. Furthermore, in the real case, there are losses at both inlet and outlet, leading to an increased value of entropy and to a lower overall efficiency. In the thermodynamic cycle of a real engine - starting from ambient conditions, where static and total pressure are the same - there is an increase in entropy during the inlet, leading to a slightly lower level of total pressure after the inlet. The same applies to outlet phase, where the nozzle induces a small loss in total pressure and gain in entropy.

The modeling process adopted for this calculation uses certain assumptions to simplify the real case, as long as the consistency with the physical phenomena and with the measured data is guaranteed. In particular, ideal gas assumption is set for all states of calculation. Furthermore, we assume an adiabatic inlet, a fixed pressure-drop during combustion and an adapted, ideal nozzle.

Ideal Gas This assumption allows to easily calculate the entropy generated as well as the energy (enthalpy) generated and absorbed during the processes. Nevertheless, being the gas ideal and not perfect the accuracy is higher, since specific heat capacities at constant pressure and volume - c_p and c_v - are constantly updated based on temperature changes.

Adiabatic, Ideal Inlet Assuming adiabatic and ideal inlet means that there are no heat additions nor losses and pressure losses at the inlet stage. As a consequence, there is no entropy generation, that is to say conditions after the inlet meet the ambient conditions: temperature and total pressure are the same. Friction losses are neglected and, being the amount of time spent by the fluid within the inlet so small, heat exchange can be neglected as well. After the inlet the fluid is slightly accelerated, so static pressure is lower than total pressure. Because only a stationary test environment is considered there is no ram effect at the inlet. Eventually, the compressor lifts the fluid up to a higher pressure level.

Pressure Drop Heat addition in the combustion chamber is not loss free. Because of this, the total pressure at the beginning of the combustion chamber is lightly lower than that at the end of the process, thus increasing the entropy of the process. The total temperature at this point is the same resulting from an isobaric process, the only difference lies in the entropy generation. Larger engines show a total pressure loss of about 2%, but given the small dimensions of the engine, a general overall pressure ratio of 0.92 during combustion is assumed.

Adapted, Ideal Nozzle First, assuming an adapted nozzle allows to state that the static pressure at the exit of the nozzle is equal to ambient pressure. Secondly, given the small size of the nozzle, it is possible to neglect pressure losses and entropy generation at this stage. Another factor that is not being considered here is the turbulence on the Boundary Layer. Consequently, there is no change in total pressure within the nozzle.

Moreover, one main issue for a realistic recalculation of the Joule-Brayton cycle is the temperature dependence of c_p and c_v, because of their significant change over the tested temperature field. For an accurate assumption, two approaches are considered: one regarding polynomial expansion with coefficients given from literature, the other based on interpolation of experimental values. In both cases the mixture of kerosene with air is treated as an ideal gas for simplification. In the end, the polynomial approach is preferred, since the absence of reliable tables for kerosene made the interpolation results inaccurate. In particular, for the polynomial approach two sources are compared, first the National Institute of Standards and Technology[4] database and secondly the coefficients taken from the book *Projektierung der Flugzeugtriebwerke*[5]. Eventually, the latter is chosen, since it provides more reliable coefficients for the air - kerosene mixture, allowing to avoid evaluating the components separately.

By inserting all the obtained data for every engine speed in a Matlab code a cycle graph is obtained, as shown in Figure 9, where the entropy is evaluated via the ideal gas assumption, with an initial value assumed equal to zero.

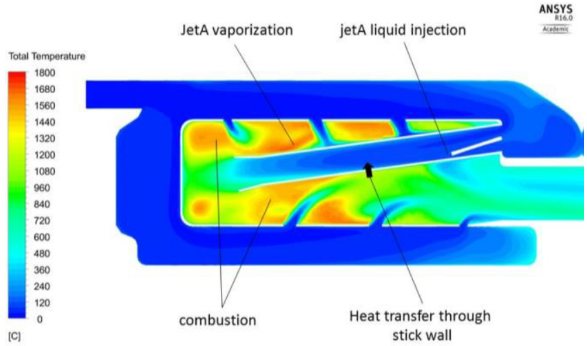

Figure 10: *Temperature Distribution within the Combustion Chamber, from [6]*

7 Discussion

There are two evident conclusions from Figure 9, showing the recreated thermodynamic cycle. Firstly, turbine entry temperature is too high, and secondly, entropy values decrease between the turbine inlet and outlet, casting doubts on the accuracy of some of the measurements.

7.1 Temperature

At first there is an investigation about the high turbine entry temperature, starting with considering the material of the combustion chamber, Inconel. Inconel has its melting point at about 1500 K, and permanent temperature resistance around 1000 K [7], therefore the measured turbine entry temperature (about 1200 K) seems way to high. Also, the isentropic efficiency calculated with these turbine entry temperatures lays at about 3.14 which is actually not reasonable.

It is therefore assumed that turbine entry temperature is most likely to be inaccurately recorded. A possible explanation for this might be the specific structure of the combustion chamber. In this reverse flow combustion chamber small tubes are used for first inserting the liquid fuel and then vaporizing it. A vortex motion is holding the hot primary combustion flame at the end of the tube, whilst in the surrounding of the tube the combustion is significantly colder. Taking a closer look at the temperature difference among the sticks, as suggested from [6] there are peaks up to 400 degrees. This means that placing a sensor in a slightly different position might result into a totally different measurement. Because of this, it's prone to conclude that total temperature after combustion is in fact wrong, and therefore needs to be measured again or recalculated.

The isentropic efficiency of the compressor calculated out of the measured temperatures (87%) and the compressor's pressure ratio 1.8 seem reasonable according to [3]. Therefore, one approach is now to recalculate the total temperature after combustion differently, at first via the power balance of the turbine shaft, a mechanical connection always valid. For all further recalculation, only engine speed at 100000 rpm is considered, since sensor errors are presumed to be less pronounced at higher engine speed. The recalculated value for turbine entry temperature is approximately 840 K, with a consequent turbine isentropic efficiency of 65%. Larger engines found in civil aircraft application have an isentropic efficiency at about 90% [5], therefore given the smaller scale of the model gas turbine, 65% seems reasonable.

	Before recalculation [%]	After recalculation [%]
$\eta_{\text{is, compressor}}$	83.3	83.3
$\eta_{\text{is, turbine}}$	320.7	69

Table 1: *Efficiencies Recalculation*

7.2 Thrust

Further more, it is evident from the Figure 12 that the calculated thrust is approximately 1.4 times lower that that measured, which is likely unrelated to the turbine inlet temperature measurement since the thrust calculation is not directly dependent on that. Thrust calculation is only dependent on the outlet speed and mass flow – the pressure term in thrust equation is neglected since the nozzle is adapted. The next suspected measurement is the air volumetric flow. This is due to the fact that it is not measured directly and it depends strongly on calibration, which in this case was performed elsewhere than the experiment at unknown ambient conditions.

This hypothesis is investigated by determining the Mach number corresponding to the measured thrust, outlet geometry, isentropic exponent and ambient pressure – all of which are variables with higher confidence factor than the airflow. Subsequently, an outlet speed is determined based on the measured outlet temperature, yielding a result 30% higher than that calculated previously based on the measured values. The significant influence of outlet temperature measurement is ruled out using a simple sensitivity study (Figure 11). Therefore, air volumetric flow measurement remains the likely most significant contributing factor to the thrust calculation versus measurement discrepancy.

As a result, a correction factor based on the outlet speed discrepancy was introduced to recalculate the thrust with more realistic results, as shown in Figure 12.

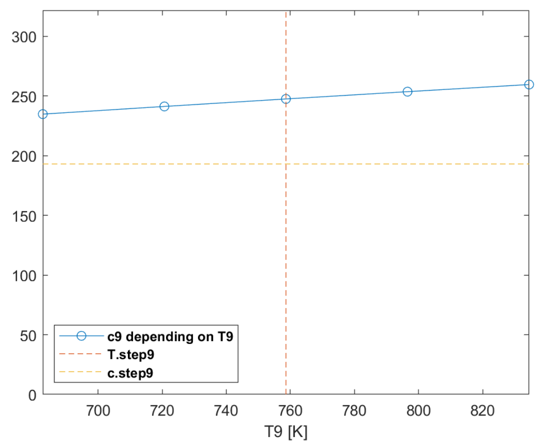

Figure 11: *Sensitivity Study of the Speed at the Nozzle*

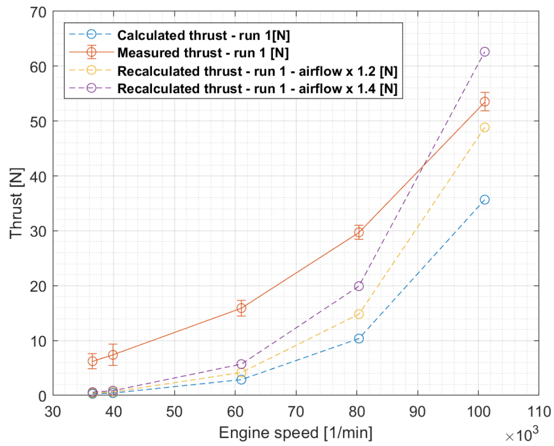

Figure 12: *Thrust measurement, calculation and recalculation comparison*

8 Conclusions

After collecting experimental data from the examined TJ 70 micro turbine and recalculating its thermodynamic cycle including calculated thrust, component efficiencies and overall efficiencies, the measured data were critically examined to most likely include systematic errors. Two main hypothesis regarding turbine inlet temperature and air volumetric flow measurements were presented to explain these phenomena, further supported by investigation of possible causes and recalculation using derived corrections to relate back to the measured data. The main likely sources of error are the uneven distribution of temperature within the combustion chamber and indirect measurement of volumetric flow combined with possible calibration issues.

As a result, the main takeaway for similar experiments is to implement more robust measuring techniques – particularly for example using more probes, so that the data obtained is more representative of real situation within the engine.

Regarding recommendations for improvements on the micro turbine itself – and to stay away from the obvious such as increase in size or heightening the overall compression ratio to achieve better efficiency and/or performance – one aspect potentially worth of further investigation is adjusting air-fuel ratio and the relevant temperature margins at the turbine inlet. The recalculated values of temperature at that point suggest conservatism of the design. It needs be stressed however that the engine was not run at full speed and this is therefore mere recommendation for further investigation, which would nevertheless be closely linked with the issue encountered during this experiment – the true temperature distribution behind the combustion chamber.

Bibliography

[1] *Skript Modul Flugantriebe*.

[2] R. Decuypere D. Verstraete. *Micro Turbines from Standpoint of Potential Users*. 2005.

[3] *http://www.rc-network.de/forum/showthread.php/11006-TJ-70-18-Raptor*.

[4] *NIST, National Institute of Standards and Technology*.

[5] H. Grieb. *Projektierung von Flugzeugtribwerken*. 2004.

[6] F. Fuchs V. Meidinger N. Neuburger T. Reiter M. Zuendel A. Hupfer. *Challenges in designing very small jet engines, fuel distribution and atomization*. 2016.

[7] *https://cdn2.hubspot.net/hubfs/483909/Corrotherm-Oct2016-Theme/PDF%20Files/Inconel*$_{a}lloy_{6}25.pdf$.

Appendices

A Abbreviations

ECU	Engine Control Unit
EGT	Exhaust Gas Temperature
RC	Radio Controlled
c_p	Specific heat capacity at constant pressure
c_v	Specific heat capacity at constant volume

Table 2: *Abbreviations*

B Matlab results

RESULTS - MEASURED DATA
speed
0-10.8194-0-0-16.0312-
0-12.909-0-0-19.5084-
0-31.3036-0-0-52.053-
0-58.389-0-0-102.5993-
0-114.0391-0-0-192.9805-
entropy
0-16.881-20.1316-1512.6683-1131.622-
0-16.881-17.9922-1503.5021-1123.3033-
0-16.881-23.0988-1492.594-1108.6979-
0-16.881-30.9998-1452.845-1122.2939-
0-16.881-50.3505-1463.6459-1084.6591-
total temperature
278.75-278.75-287.8531-1018.2299-752.9781-
278.75-278.75-288.6484-1024.4231-752.1773-
278.75-278.75-300.7717-1086.1697-761.6032-
278.75-278.75-317.7361-1114.5433-784.0688-
278.75-278.75-345.0572-1202.8701-778.4117-
static temperature
278.75-278.6917-0-0-752.7709-
278.75-278.667-0-0-751.8854-
278.75-278.2621-0-0-759.912-
278.75-277.0526-0-0-778.118-
278.75-272.2752-0-0-758.6275-
total pressure
96900-96900-107223.903-98645.9907-96981.4802-
96900-96900-109076.5137-100350.3926-97017.046-
96900-96900-123769.7586-113868.1779-97626.588-
96900-96900-145957.2491-134280.6691-99502.6709-
96900-96900-182306.1066-167721.618-105985.0831-
static pressure
96900-96829.0674-0-0-96900-
96900-96799.0446-0-0-96900-
96900-96308.4966-0-0-96900-
96900-94864.0882-0-0-96900-
96900-89448.7117-0-0-96900-
air
0.9101-0.91968-0.95511-0.96981-0.97925-
fuel
0.0899-0.080324-0.044891-0.030192-0.020748-
compressor efficiency
0.83296
turbine efficiency
3.2065

RESULTS - MEASURED DATA, Tt,4 AND MASSFLOW CORRECTION
speed
0-12.9833-0-0-19.8335-
0-15.4908-0-0-24.0918-
0-37.5643-0-0-63.5466-
0-70.0667-0-0-123.6988-
0-136.8469-0-0-226.2174-
entropy
0-16.881-20.1316-1128.0959-1115.6725-
0-16.881-17.9922-1117.325-1107.4728-
0-16.881-23.0988-1097.6109-1093.582-
0-16.881-30.9998-1081.9701-1107.3403-
0-16.881-50.3505-1026.9069-1065.7167-
total temperature
278.75-278.75-287.8531-763.7-752.9781-
278.75-278.75-288.6484-764.4-752.1773-
278.75-278.75-300.7717-793.3-761.6032-
278.75-278.75-317.7361-824.4-784.0688-
278.75-278.75-345.0572-838.3-778.4117-
static temperature
278.75-278.6661-0-0-752.6834-
278.75-278.6305-0-0-751.7616-
278.75-278.0475-0-0-759.1928-
278.75-276.3058-0-0-775.6871-
278.75-269.4263-0-0-751.7821-
total pressure
96900-96900-107223.903-98645.9907-97019.1294-
96900-96900-109076.5137-100350.3926-97071.08-
96900-96900-123769.7586-113868.1779-97954.5172-
96900-96900-145957.2491-134280.6691-100622.5793-
96900-96900-182306.1066-167721.618-109340.1642-
static pressure
96900-96797.8806-0-0-96900-
96900-96754.6718-0-0-96900-
96900-96049.8666-0-0-96900-
96900-93987.5255-0-0-96900-
96900-86423.4247-0-0-96900-
air
0.92393-0.93213-0.96224-0.97455-0.98224-
fuel
0.076073-0.067866-0.037761-0.02545-0.017762-
compressor efficiency
0.83296
turbine efficiency
0.69081
combustion efficiency
0.79455
cycle efficiency
0.066309

Step	Assumptions	Calculations
Inlet	Tt.step0=T.step0=Tt.step2 area.step2 vflow.step2 pt.step0=p.step0=pt.step2	p.step0,T.step0 $\Rightarrow \rho.step0$ area.step2,vflow.step2 $\Rightarrow c.step$ Tt.step2,c.step2,cp.step2 $\Rightarrow T.step2$ pt.step2,c.step2,T.step2 $\Rightarrow p.step2$ p.step2,T.step2 $\Rightarrow \rho.step2$ vflow.step2,$\rho.step2 \Rightarrow massflow$ Tt.step2,pt.step2 $\Rightarrow s.step2$
Compressor	pt.step3 Tt.step3 k.step3	pt.step3,Tt.step3,pt.step2,Tt.step2 $\Rightarrow Tis.step3, s.step3$ Tt.step3,Tis.step3,Tt.step2 $\Rightarrow \eta_{\text{is, comp}}$
Combustion	Tt.step4 k.step4 $\text{vflow}_{\text{fuel}}$ ρ_{fuel} pressure ratio Hi_{fuel}	$\text{vflow}_{\text{fuel}}$,$\rho_{\text{fuel}} \Rightarrow mflow_{\text{fuel}}$ $\text{mflow}_{\text{air}}$,$\text{mflow}_{\text{fuel}} \Rightarrow air[\%], fuel[\%]$ pt.step3,pressure ratio $\Rightarrow pt.step4$ pt.step4,Tt.step4,pt.step3,Tt.step3 $\Rightarrow s4$ Tt.step3,Tt.step4,Hi_{fuel},mflow $\Rightarrow \eta_{\text{combustion}}$
Turbine and Nozzle	Tt.step9 area.step9	mflow,area.step9,p.step9,Tt.step9 $\Rightarrow T.step9$ T.step9,p.step9 $\Rightarrow \rho.step9$ mflow,area.step9,$\rho.step9 \Rightarrow c.step9$ p.step9,$\rho.step9, c.step9 \Rightarrow pt.step9$ Tt.step9,pt.step9,Tt.step4,pt.step4 $\Rightarrow s9, Tis.step9$ Tis.step9,Tt.step9,Tt.step4 $\Rightarrow \eta_{\text{is, turbine}}$ mflow,c.step9,c.step0 $\Rightarrow thrust$

Table 3: *Matlab Workflow*